

# Chemoenzymatic Synthesis and Study of Poly( $\alpha$ -methyl- $\beta$ -propiolactone) Stereocopolymers

Jin Xu<sup>†</sup> and Richard A. Gross\*

Department of Chemistry, University of Massachusetts—Lowell, One University Avenue, Lowell, Massachusetts 01854

David L. Kaplan

RD&E Center, Biotechnology Division, STRNC-YM, U.S. Army Natick, Natick, Massachusetts 01760-5020

Graham Swift

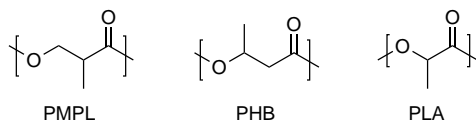
Rohm & Haas Company, Spring House, Pennsylvania 19477

Received December 18, 1995; Revised Manuscript Received March 21, 1996<sup>®</sup>

**ABSTRACT:** A chemoenzymatic route from racemic  $\alpha$ -methyl- $\beta$ -propiolactone (MPL) to optically active (*R*)-poly( $\alpha$ -methyl- $\beta$ -propiolactone), (*R*)-PMPL, was demonstrated which involved lipase catalyzed resolution of MPL enantiomers in organic media and subsequent chemical polymerization. From a comparative study of different enzymes and organic media, catalysis by the lipase PS-30 from *Pseudomonas fluorescens* suspended in diethyl ether was found to be most suitable for MPL enantioselective alcoholysis reactions. MPL having up to 93% (*R*) content was thus obtained, mixed in various proportions with racemic MPL, and polymerized using  $\text{CH}_3\text{COOK}$ /dibenzo-18-crown-6. From a plot of specific rotation vs % enantiopurity, it was estimated that the  $[\alpha]_D^{25}$  for 100% (*R*)-PMPL is  $-38.4^\circ$  ( $c$  0.8 g/dL,  $\text{CHCl}_3$ ).  $^{13}\text{C}$  NMR analysis (62.9 MHz) provided information on triad sequence distributions from observation of methine carbons, while the methyl and carbonyl carbons were sensitive to diad sequences. The polymerization of 50% (*R*)-MPL followed Bernoulli random chain propagation statistics. In contrast, polymerizations of 74% and 93% (*R*)-MPL deviated from the Bernoulli model. Further analysis showed that these latter polymerizations fit the enantiomeric-site model. Thus, isoregulating characteristics of the  $\text{CH}_3\text{COOK}$ /dibenzo-18-crown-6 catalyst for enantioenriched MPL polymerizations were demonstrated. By increasing the % (*R*)-content in the monomer feed to 93%, a product was obtained which, by DSC, had  $T_m$  and  $\Delta H_f$  values of  $131^\circ\text{C}$  and 22.0 cal/g, respectively. Furthermore, WAXS analysis carried out on a melt-annealed 90% (*R*)-PMPL sample showed that the polymer was highly crystalline (approximately 73%). FTIR analysis was used to identify vibrational bands at 997, 1010, 1059, 1185, 1249, and  $1334\text{ cm}^{-1}$  which were crystalline-sensitive, while the band at  $1465\text{ cm}^{-1}$  was crystalline-insensitive.

## Introduction

Poly( $\alpha$ -methyl- $\beta$ -propiolactone), PMPL, is intriguing since it is closely related in structure to microbial poly(3-hydroxybutyrate), PHB, and poly(lactide), PLA.



Poly((*R*)-3-hydroxybutyrate) and related microbial polyesters have proved of great interest as candidates for bioerodable medical implants and as materials which are mineralized by microorganisms upon exposure to various ecosystems (biodegradable polymers).<sup>1</sup> PLA and related copolyesters are being used and continue to be studied as bioerodable plastics for medical applications.<sup>2,3</sup> Furthermore, PLA copolyesters have recently gained considerable attention as biodegradable polymers for environmental technologies.<sup>4,5</sup> Thus, it appears interesting to explore the potential utility of PMPL for applications where PHB and PLA have shown promise. However, it became apparent to us based on literature reviews that research was needed for the preparation of PMPL having high enantiopurity.

Several optically active poly( $\alpha$ -substituted  $\beta$ -propiolactones) have been prepared via ring-opening polymerization of enantioenriched lactone monomers. Examples include poly( $\alpha$ -phenyl- $\beta$ -propiolactone),<sup>6</sup> poly( $\alpha$ -ethyl- $\alpha$ -phenyl- $\beta$ -propiolactone),<sup>7,8</sup> and poly( $\alpha$ -methyl- $\alpha$ -ethyl- $\beta$ -propiolactone).<sup>9</sup> These reports share the common feature that the chiral monomers were via tedious multistep synthetic schemes. The resolution of lactone precursor enantiomers involved the formation of diastereomeric salts and multiple recrystallizations. For PMPL, monomers enriched in either (*R*)- or (*S*)- $\alpha$ -methyl- $\beta$ -propiolactone, MPL, were synthesized from the chiral precursors (*R*)- and (*S*)-methyl 3-hydroxy-2-methylpropionate by reaction with hydrobromic acid to form the corresponding 3-bromo derivatives and subsequent ring closure under basic conditions.<sup>10</sup> Difficulties were encountered such as low optically active MPL yields ( $\sim 13\%$  from methyl 3-hydroxy-2-methylpropionate) and loss in enantiopurity relative to the starting chiral synthon (see the Results and Discussion section, below).<sup>10</sup>

Commercially available enzymes have proven to be powerful tools for the resolution of racemic mixtures to obtain products in high enantiopurity.<sup>11</sup> Lipases such as porcine pancreatic lipase (PPL), pig liver esterase (PLE), horse liver esterase (HLE), *Pseudomonas fluorescens* lipase PS-30, and the lipase from *Candida cylindracea* (CC) have been widely used for the resolution of racemic alcohols and carboxylic acids by catalyzing enantioselective esterification/transesterification

\* Corresponding author.

<sup>†</sup>This paper is part of the thesis dissertation of Jin Xu, University of Massachusetts—Lowell, 1995.

<sup>®</sup> Abstract published in *Advance ACS Abstracts*, May 15, 1996.

reactions. Successful examples of  $\gamma,\delta,\epsilon$ -lactone resolutions in aqueous media by using PLE, PPL, and HLE lipases have been reported.<sup>12–14</sup> The use of enzymes in organic media have shown promising substrate conversion efficiency and high enantioselectivity and offer advantages relative to reactions in aqueous media such as catalyst recyclability, increased enzyme thermal stability, solubility of a wide range of substrate types in the reaction media, and no requirement for pH adjustment as the reaction proceeds.<sup>15,16</sup> Lipases in organic media have been used successfully for the preparation of enantioenriched  $\gamma$ -butyrolactones,  $\omega$ -lactones, and  $\delta$ -lactones by lactonization of racemic  $\gamma$ -hydroxy esters,  $\omega$ -hydroxy esters, and  $\delta$ -hydroxy esters, respectively.<sup>17–19</sup>

In this work, a model study was carried out to determine the utility of enzyme catalysis in organic media for the resolution of substituted  $\beta$ -propiolactones enantiomers. The resulting enantioenriched lactones could then be polymerized via chemical methods to form substituted poly- $\beta$ -esters having the desired stereochemical configuration. This would be a chemoenzymatic strategy that has proved useful in other systems such as for the preparation of polyvinyls with sugar pendant groups.<sup>20</sup> For this study, we chose the lactone MPL and lipases PPL, PS-30, and CC. The effect of the PS-30–organic solvent pair used on the rate of MPL reactivity and enantioselectivity was determined. Using enantioenriched MPL prepared by enzymatic resolution, PMPL stereoisomers were prepared. <sup>13</sup>C nuclear magnetic resonance (NMR) was used to study the repeat unit sequence of polymers on diad and triad levels. The effect of PMPL enantiopurity on solid-state thermal transitions, percent crystallinity, and vibrational bands was studied by differential scanning calorimetry (DSC), wide angle X-ray scattering (WAXS), and Fourier transform infrared spectroscopy (FTIR). Also, the relationship between polymer enantiopurity and the specific rotation was investigated.

## Experimental Section

**Materials.** Porcine pancreatic lipase Type II (PPL), *Candida cylindracea* lipase Type VII (CC), and *p*-nitrophenyl acetate were purchased from Sigma Chemical Co., and *Pseudomonas fluorescens* lipase PS-30 was from Amano Enzyme USA. All the enzymes were used as received. Measurements of esterase activity for these enzymes in organic media are described below.

The solvents methanol, *n*-hexane, diethyl ether, 1,4-dioxane, ethyl acetate, and benzene were purchased from Aldrich (reagent grade, >99% purity). They were dried by reflux over CaH<sub>2</sub> overnight prior to distillation under argon. The values for water contents of the dried solvents were determined using a Karl Fischer automatic titrator as was described elsewhere<sup>21</sup> and were found to be 39 ± 5, 55 ± 4, 160 ± 11, 84 ± 4, 57 ± 5, and 98 ± 9 ppm for *n*-hexane, diethyl ether, 1,4-dioxane, ethyl acetate, benzene, and methanol, respectively. Methacrylic acid was obtained from Aldrich and purified by fractional distillation (71–72 °C/60 mmHg). Hydrobromic acid was obtained from Aldrich as a 30 wt % solution in acetic acid and used as received.

**Preparation of *rac*- $\alpha$ -Methyl- $\beta$ -propiolactone (MPL).** The method used is a modification of that previously described.<sup>10</sup> Into 86 g (1.0 mol) of methacrylic acid cooled by an external ice–water bath and stirred magnetically was added over a 15-min period 270 g of a cooled 30 wt % hydrobromic acid in acetic acid solution (1.0 mol of HBr). The ice bath was then taken away, and the mixture was stirred in the dark at ambient temperature for 2 days, after which the remaining HBr was removed by a water pump followed by fractional distillation of 3-bromo-2-methylpropionic acid (86–87 °C/1.2

mmHg) to give 152 g (91% yield) of 3-bromo-2-methylpropionic acid: <sup>1</sup>H NMR  $\delta$  1.34 (d, 3 H), 2.94 (m, 1 H), 3.48 (m, 1 H), 3.58 (m, 1 H), 11.70 (br s, 1 H). To synthesize MPL, 20 g (0.12 mol) of 3-bromo-2-methylpropionic acid was mixed with 20 mL of distilled water in an ice-bath. With the mixture at a temperature below 10 °C, saturated sodium bicarbonate solution was added so that the pH was approximately between 7.4 and 7.8. Chloroform (200 mL) and (C<sub>4</sub>H<sub>9</sub>)<sub>4</sub>NBr (0.386 g, 1 mol %) were then added. The resultant biphasic mixture was stirred vigorously at approximately 15 °C for 12 h. The CHCl<sub>3</sub> phase was then separated, washed 2 times with 50-mL portions of distilled water, and dried over anhydrous Na<sub>2</sub>SO<sub>4</sub>, and the solvent was removed by rotary evaporation. To avoid severe losses in yields, the crude product was then immediately distilled using a short-path distillation head (external oil bath temperature ~45 °C, ~2 mmHg) to give 4.10 g (40% yield) of a colorless liquid that, based on <sup>1</sup>H NMR, appeared to be >95% pure. Prior to use of the monomer for polymerization reactions, it was fractionally distilled from CaH<sub>2</sub> (46 °C/4.5 mmHg) under argon. The <sup>1</sup>H NMR and IR spectra are consistent with that previously reported.<sup>10</sup>

**Assay of PPL, PS-30, and CC Activity.** The enzymes were assayed using *p*-nitrophenyl acetate (pNPA) and methanol in 1,4-dioxane. A 1,4-dioxane solution (5 mL) containing pNPA (1.45 mmol/L) and methanol (2.82 mmol/L) was added to 10-mL vials containing approximately 17 mg of enzyme. The assay reactions were carried out for 2 h in an orbital shaker (200 rpm, 35 °C) and were terminated by removal of the enzyme by filtration. The concentration of the reaction product *p*-nitrophenol (pNP) was determined by UV–vis (GBC UV/vis 916) at the  $\lambda_{\text{max}}$  (305 nm) of pNP. Since both pNP and pNPA contribute to the measured absorbance (*A*) at 305 nm, the equation below was used to calculate the concentration of pNP at this wavelength:<sup>22</sup>

$$C_{\text{pNP}} = (A - \epsilon_{\text{pNPA}}C)/(\epsilon_{\text{pNP}} - \epsilon_{\text{pNPA}}) \quad (1)$$

where  $C_{\text{pNP}}$  and  $C_{\text{pNPA}}$  are concentrations (in mol/L) of pNP and pNPA, respectively,  $\epsilon_{\text{pNP}}$  and  $\epsilon_{\text{pNPA}}$  are the extinction coefficients of pNP and pNPA, respectively (determined to be 11 000 and 2100 L/(mol·cm), respectively, at  $\lambda = 305$  nm), and  $C$  is equal to  $C_{\text{pNP}} + C_{\text{pNPA}}$ , which is equivalent to the initial  $C_{\text{pNPA}}$  concentration. Enzyme activities for PPL, CC, and PS-30 are defined herein as the nanomoles of pNPA hydrolyzed in dioxane per unit weight of enzyme per minute (nmole pNP/(min·mg)) and have values of 1.2, 1.2, and 3.0, respectively.

**Enzymatic Resolution of MPL.** All glassware was oven-dried at about 150 °C overnight and then cooled in a desiccator (containing Drierite) prior to use. For studies to determine the effects of solvent and enzyme on monomer conversion and enantioselectivity, methanol was used as the nucleophile. The enzymes were transferred in a drybag containing Drierite as desiccant under an argon purge. Liquids were transferred via syringe under an argon atmosphere. MPL (300 mg, 3.49 mmol), anhydrous methanol (223 mg, 6.97 mmol), and 3.8 mL of solvent were added into 8-mL vials which contained 174 mg of enzyme. The reaction vials were capped, magnetically stirred, and maintained at 35 °C for reaction times as specified below. The reactions were terminated by removing the enzymes by filtration using a 0.45- $\mu$ m Teflon syringe filter, and MPL conversions were determined by FTIR as described below. After concentration of solutions by rotoevaporation at room temperature, the enantioenriched MPL was separated from the reaction mixtures by column chromatography (column dimensions of 2.5 cm by 24 cm) using silica gel (purchased from Aldrich, grade 60, Merck, 230–400 mesh, 60 Å) as the stationary phase and methylene chloride as the eluent with a flow rate of ~2 mL/min and a ratio of ~200:1 silica gel to mixture. The major fractions containing MPL eluted at volumes between 80 and 100 mL. Larger scale resolution of MPL (20.0g, 0.233 mol) was carried out using the lipase PS-30, dry diethyl ether as solvent, and dry benzyl alcohol (Eastman Kodak, 99+% purity, distilled from CaH<sub>2</sub>) in place of methanol with the same relative molar ratios of reagents and similar precautions to avoid water that were described above. The resolution was carried out in a three-neck 500-

mL round-bottom flask at 25 °C for 9 days. The workup involved removal of enzyme by filtration, solvent rotoevaporation at 25 °C, and distillation both in the absence and presence of CaH<sub>2</sub> as described above for racemic MPL. The product (yield 25%) had a  $[\alpha]_D^{25} +15.3^\circ$  (*c* 1.0 g/dL in CHCl<sub>3</sub>) which, based on a value of +18.0° for enantiopure (*R*)-MPL (see Results and Discussion section, below), indicates a 93% (*R*) content.

**Polymerization of MPL Monomer of Variable Enantiopurity.** The initiator CH<sub>3</sub>COOK/dibenzo-18-crown-6 (19.0 mg containing 0.0230 mmol of CH<sub>3</sub>COOK and 0.0464 mmol of dibenzo-18-crown-6; see below for preparation) was transferred in a drybag containing Drierite with constant argon purging into flame-dried 3-mL ampules. The ampules were then capped, removed from the glovebox, and placed under a positive argon atmosphere, and MPL (1.00 g, 0.0116 mol) was added via syringe. Reaction ampules were then mixed thoroughly using a vortexer and placed into an oil bath at 60 °C. The reactions were terminated by dissolving the reaction contents into CHCl<sub>3</sub> (5 mL) and adding the chloroform solution into methanol (100 mL) to precipitate the polymer which was separated by vacuum filtration and then dried in a vacuum oven (50 °C, 0.5 mmHg, 24 h) prior to characterization: <sup>1</sup>H and <sup>13</sup>C NMR spectra of the polymer products were consistent with that expected (see Figures 4–6).

**Preparation of Polymerization Initiator CH<sub>3</sub>COOK/Dibenzo-18-crown-6.** The method used was a modification of that previously described.<sup>23</sup> All transfers of solids were in a drybag containing Drierite with constant argon purging, while liquids were transferred via syringe under a positive argon atmosphere. To a previously silanized and flame-dried 50-mL flask was added dry methanol (50 mL), CH<sub>3</sub>COOK (19.1 mg, 0.195 mmol), and dibenzo-18-crown-6 (145 mg, 0.402 mmol). The resulting mixture was refluxed for 1 h under argon, the methanol removed by sparging with dry argon, and the resulting solid dried using a drying pistol (100 °C, 10 μmHg, 48 h).

**Instrumentation Methods.** FTIR (Mattson Instruments Galaxy Series 2020) was used to determine lactone conversions to their corresponding methyl esters. Calibration curves (correlation coefficients of higher than 0.993) were obtained by dilute solution measurements in CCl<sub>4</sub> using a series of MPL/methyl 3-hydroxy-2-methylpropionate mixtures of known composition and measuring the ratio of lactone (1845 cm<sup>-1</sup>) to ester carbonyl group (1735 cm<sup>-1</sup>) absorptions in a solution cell (6-mm path length). For reactions in hexane, 1,4-dioxane, and diethyl ether, sufficient quantities of the reaction mixtures (~20 μg) were added to CCl<sub>4</sub> (~3 mL) so that the transmittance of the lactone absorption band was ~30%. When using ethyl acetate and benzene, solvent absorptions in the regions of interest interfered so that solvent removal at 25 °C by rotoevaporation was carried out prior to addition of the lactone/methyl ester mixture to CCl<sub>4</sub>.

The enantiomeric excess (ee) of resolved lactones that were purified by either column chromatography or distillation (see above) was determined by <sup>1</sup>H NMR (see below) and polarimetry. For the latter, measurements of optical rotation were obtained using a Perkin-Elmer 241 polarimeter at 25 °C and are reported as follows:  $[\alpha]_D^{25}$  = specific rotation (*c* is concentration in grams per 100 mL of solvent).

<sup>1</sup>H NMR spectra were recorded on either Bruker WP-270 SY or Bruker AMX-250 spectrometers at 270 and 250 MHz, respectively. Polymers were analyzed at 4% (w/v) in CDCl<sub>3</sub>. Determinations of MPL enantiopurity by <sup>1</sup>H NMR were carried out using approximately 0.5% (w/v) MPL in CDCl<sub>3</sub> and 40 mol % (relative to MPL) europium(III) tris[3-((heptafluoropropyl)-hydroxymethylene)-(+)-camphorate] (Eu-(+)-[hfc]<sub>3</sub>) as the chiral chemical shift reagent. The relative peak areas of MPL stereoisomers were measured by peak curve fitting and the cut/weight method. <sup>1</sup>H NMR chemical shifts in parts per million (ppm) were recorded using tetramethylsilane (TMS) as an internal reference at 0.00 ppm. Experimental parameters for <sup>1</sup>H NMR spectra of polymers were as follows: pulse width 4.9 μs (30°); relaxation delay 0.50 s; 32K data points; and 128–256 transients. Experimental parameters for <sup>1</sup>H NMR spectra recorded of monomers with and without Eu-(+)-

[hfc]<sub>3</sub> were as follows: pulse width 2 μs; relaxation delay 0.50 s; 16K data points; and 32 transients. <sup>13</sup>C NMR spectra were recorded on a Bruker AMX-250 spectrometer at 62.9 MHz, and the chemical shifts in ppm were recorded using CDCl<sub>3</sub> as the reference at 77.00 ppm. Experimental parameters for <sup>13</sup>C NMR spectra were as follows: polymer concentration 4% (w/v); pulse width 6.3 μs; acquisition time 1.6 s; relaxation delay 1 s; 64K data points and 11 000–13 000 transients. In order to resolve the peaks corresponding to the diad and triad chain sequences, a line broadening of –0.5 and a Gaussian multiplication function of 0.5 were used.

All thermal characterizations were carried out using a Du Pont 2910 differential scanning calorimetry (DSC) equipped with a TA 2000 data station, using between 5.0 and 8.0 mg of sample sealed in aluminum pans and a dry nitrogen purge. The polymer samples were heated at a rate of 10 °C/min from –80 to 140 °C, rapidly quenched from the melt using liquid nitrogen, and then analyzed during second heating scans from –80 to 140 °C. Data reported for the melting temperature (*T*<sub>m</sub>) and enthalpy of fusion ( $\Delta H_f$ ) were taken from the first heating scans. Where multiple melting transitions were observed, the reported *T*<sub>m</sub> was the peak melting temperature of the largest endotherm transition.  $\Delta H_f$  values were taken as the cumulative value over the entire melting transition range. The reported glass transition temperature (*T*<sub>g</sub>) values were the midpoint values measured during the second heating scans.

Molecular weights were measured by gel permeation chromatography (GPC) using a Waters Model 510 pump, Model 410 refractive index detector, and Model 730 data module with 500-, 10<sup>3</sup>-, 10<sup>4</sup>-, and 10<sup>5</sup>-Å Ultrastaygel columns in series. Chloroform (HPLC grade) was used as an eluent at a flow rate of 1.0 mL/min. The sample concentrations and injection volumes were 0.3% (w/v) and 150 μL, respectively. Polystyrene standards with a low polydispersity (Polysciences) were used to generate a calibration curve.

FTIR spectra of 50%, 90%, and 74% (*R*)-PMPL products were recorded on a Mattson Instruments Galaxy Series 2020 at room temperature with 32 scans and 4-cm<sup>-1</sup> resolution. Approximately 1 mg of 74% and 1 mg of 90% (*R*)-PMPL were placed on a NaCl plate which was then heated (~140 °C) using a hot plate to melt the samples. Subsequently, an additional NaCl plate was compressed on top of the liquefied samples, and the hot plate was removed. The 74% (*R*)-PMPL sample was immediately placed in the FTIR spectrometer, and a spectrum was recorded (spectral acquisition time of ~1 min). A spectrum of this sample was also recorded after annealing for 20 h at ambient temperature. The 90% (*R*)-PMPL sample was annealed at ambient temperature for 1 h prior to FTIR analysis. For the 50% (*R*)-PMPL sample, ~1 mg was compressed between two NaCl plates without thermal treatment, and the spectrum was recorded.

A wide-angle X-ray scattering (WAXS) diffractogram for 90% (*R*)-PMPL was recorded on a Philips vertical diffractometer with Bragg–Brentano geometry, graphite-diffracted beam monochromator, and Cu Kα radiation (1.5405 Å). The X-ray tube was operated at 40 kV and 20 mA. The 90% (*R*)-PMPL sample used was compressed between two glass plates while melting at 140 °C for approximately 2 min. Subsequently, the liquefied sample was cooled to 100 °C and annealed for 4 h and 4 days at 100 and 25 °C, respectively. The degree of crystallinity ( $\chi_c$ ) value was determined from diffracted intensity data in the  $2\theta = 10$ –35° range according to a method described by Bloembergen *et al.*<sup>24</sup>

## Results and Discussion

**Resolution of MPL by Using CC, PPL and PS-30.** The lipase CC showed no apparent catalytic activity (by FTIR; see Experimental Section) for MPL methanolysis in diethyl ether at 35 °C for 48 h. Although investigations of CC-catalyzed resolutions in other organic media might have shown improved results, the results in diethyl ether were not promising, so our attention was then directed toward the lipase PPL.

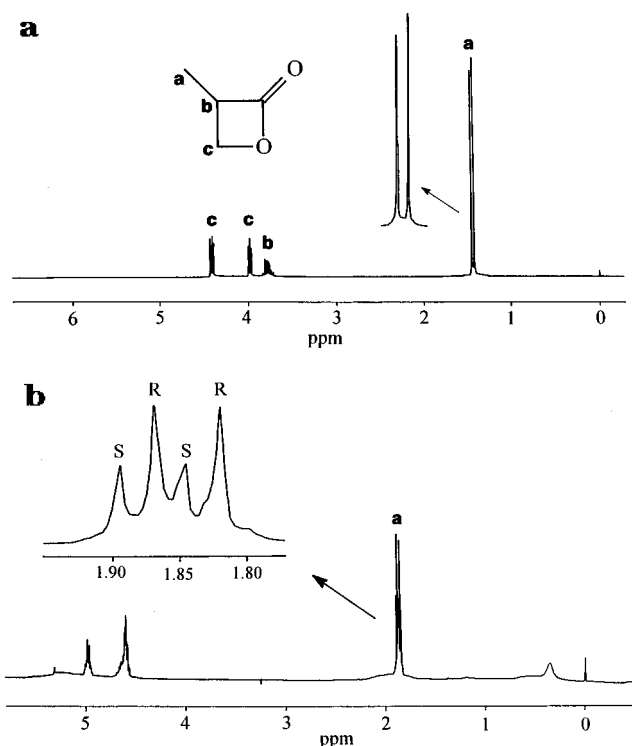


**Figure 1.**  $^1\text{H}$  NMR (250-MHz) spectra in chloroform- $d$  of 63% (*R*)-MPL recorded: (a) without Eu-(+)-[hfc] $_3$  and (b) with the addition of 40 mol % Eu-(+)-[hfc] $_3$ .

Initial investigations showed that PPL did indeed catalyze MPL methanolysis. Reactions carried out in diethyl ether, 1,4-dioxane, and ethyl acetate occurred at similar rates, reaching from 44% to 50% conversions in 48-h reaction times. MPL methanolysis occurred most slowly in benzene (20% in 48 h). When these reactions were conducted without enzyme addition, no methyl ester formation was observed (by FTIR) within a 48-h time period so that the above conversions resulted from enzyme catalysis. It is noteworthy that the catalytic activities of PPL and CC were identical (1.2 nmol of pNP/(min·mg)).

The enantiomeric ratio  $E$  is a measure of the enantioselectivity of an enzymatic transformation.  $E$  can be determined by eq 2, below, if it is assumed that A and

$$E = \frac{V_{\max A}/K_A}{V_{\max B}/K_B} = \frac{\ln[(1-c)(1-ee_s)]}{\ln[(1-c)(1+ee_s)]} \quad (2)$$

B are the fast- and slow-reacting enantiomers, respectively, that compete for the same site of the enzyme, that conversion of A and B to product is virtually irreversible, and that there is no product inhibition.<sup>25,26</sup> In eq 2,  $c$  is the conversion ( $[C_{\text{initial}} - C_{\text{final}}]/C_{\text{initial}}$ ,  $C$  is the lactone concentration) of the reaction,  $ee_s$  is the enantiomeric excess ( $[C_B - C_A]/[C_A + C_B]$ ) of the unreacted substrate, and  $V_{\max}$  and  $K$  are the maximal reaction rate and Michaelis constant, respectively. Monomer conversions were determined by FTIR (see Experimental Section). The  $ee$  values were measured from  $^1\text{H}$  NMR spectra recorded in the presence of Eu-(+)-[hfc] $_3$  (see Experimental Section). Figure 1 shows the  $^1\text{H}$  NMR spectra of an enantioenriched 63% (*R*)-MPL sample obtained by PPL-catalyzed methanolysis (22 h, 33% conversion in diethyl ether) which were recorded without and with the chiral shift reagent Eu-(+)-[hfc] $_3$ . This shift reagent resulted in almost baseline

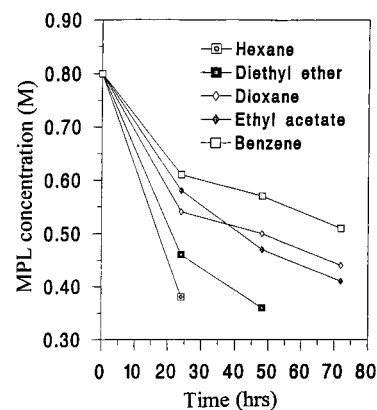


**Figure 2.** Concentration of MPL as a function of reaction time and organic media for PS-30-catalyzed MPL methanolysis.

resolution of (*R*)- and (*S*)-MPL methyl proton doublets (see Figure 1b). The upfield doublet was assigned to the (*R*)-MPL antipode based on the optical rotation measurements described below. It is noteworthy that in previous work by Hmamouchi and Prud'homme,<sup>10</sup> the chiral shift reagent 2,2,2-trifluoro-1-(9-anthryl)ethanol was used to measure MPL enantiopurity by  $^1\text{H}$  NMR but, unfortunately, poor resolution of the (*R*) and (*S*) antipodes was achieved, leading to considerable uncertainty in the monomer stereochemical purity.

Optical rotations of the enantioenriched MPL products formed by PPL resolution were positive in sign, regardless of the organic media used. Hmamouchi and Prud'homme<sup>10</sup> reported the preparation of 100% (*R*)-MPL ( $[\alpha_D^{25} + 10.5^\circ$  [ $c$  1.0 g/dL,  $\text{CHCl}_3$ ]) with retention of configuration from (*R*)-methyl 3-hydroxy-2-methylpropionate. Thus, it was concluded that PPL resolution resulted in (*R*)-MPL, where (*S*)-MPL is the more reactive enantiomer (A).

Using eq 2 and a curve-fit program, values of  $E$  were determined.<sup>27</sup> The  $E$  values for PPL-catalyzed MPL resolution in diethyl ether, benzene, ethyl acetate, and 1,4-dioxane were  $3.93 \pm 0.26$ ,  $2.98 \pm 0.24$ ,  $2.99 \pm 0.33$ , and  $2.52 \pm 0.06$ , respectively. Although the results obtained in diethyl ether were promising, higher  $E$  values were desired. Thus, investigations were initiated using the lipase PS-30.

The effects of the organic solvent used on MPL conversion for PS-30-catalyzed MPL methanolysis are shown in Figure 2. Interestingly, PS-30-catalyzed conversions after 48 h in diethyl ether and benzene were 55% and 29%, respectively, which is similar to conversions from PPL catalysis (50% and 19%, respectively) under identical conditions. Since the activity of PS-30 is 2.50 times greater than PPL for the hydrolysis of pNPA (see Experimental Section), PS-30 does not prove advantageous relative to PPL for monomer methanolysis. The important difference between PPL- and PS-30-catalyzed methanolysis of MPL is that the latter enzyme shows substantially higher enantioselectivity. This is true regardless of the solvent used (see Table 1 and above). The absolute configuration of the enantioenriched MPL stereoisomer (slower reacting enantiomer) in all of the solvents investigated was (*R*) based on measurements of optical rotation (see discussion above). The highest  $E$  values for PS-30 MPL resolutions were obtained when using benzene and diethyl ether as organic media (18 and 8.1, respectively). Considering the reaction rates and enantioselectivity, diethyl ether was chosen herein as the preferred solvent for the preparation of (*R*)-enriched MPL. It is noteworthy that

**Table 1. Enantioselectivity of the PS-30-Catalyzed MPL Methanolysis in Different Solvents<sup>a</sup>**

solvent	convsn, <sup>b</sup> %	ee, <sup>c</sup> %	<i>E</i> <sup>d</sup>
benzene	36	47	18
diethyl ether	55	72	8.1
1,4-dioxane	45	48	6.1
ethyl acetate	49	52	5.5

<sup>a</sup> 35 °C, [CH<sub>3</sub>OH]/[MPL] = 2 (molar ratio), reaction time was adjusted so that conversion was between 35% and 50%; see Experimental Section for a detailed description of the reaction conditions. <sup>b</sup> Determined by FTIR. <sup>c</sup> Determined by <sup>1</sup>H NMR with chemical shift reagent Eu-(+)-[hfc]<sub>3</sub>. <sup>d</sup> Enantioselectivity calculated by eq 2.

MPL resolution by PS-30 in hexane resulted in the formation of substantial quantities of oligomer and, therefore, was not used in this work where the desired outcome was the formation of enantioenriched lactone and methyl ester. Oligomer formation in hexane was similarly observed for resolutions conducted using PPL. These findings stimulated an investigation of enzyme-catalyzed MPL stereoselective polymerization which is described elsewhere.<sup>28</sup>

For the preparation of enantioenriched MPL for subsequent polymerization (see below), MPL was resolved by alcohololysis with benzyl alcohol using PS-30 in diethyl ether (see Experimental Section). The use of benzyl alcohol in place of methanol facilitated separation of unreacted lactone and ester by distillation. In this way, (*R*)-enriched MPL having an ee value of 86% (93% *R*) was prepared (see Experimental Section).

A plot was constructed of  $[\alpha]^{25}_D$  (*c* 1.0 g/dL, CHCl<sub>3</sub>) vs % (*R*) for MPL stereochemical mixtures (% (*R*) contents of 50%, 58%, 71%, 74%, and 90%, plot not shown). Extrapolation of the line generated by linear regression (correlation coefficient of 0.998) to 100% (*R*) gave a value of +18.0°. In previous work by Hmamouchi and Prud'homme, the reported  $[\alpha]^{25}_D$  for enantiopure (*R*)-MPL was +10.5° (*c* 1.0 g/dL in CHCl<sub>3</sub>).<sup>10</sup> The discrepancy between these values is likely due to an overestimation of the enantiopurity of MPL samples synthesized in their work. This overestimation likely resulted from poor resolution of corresponding enantiomer <sup>1</sup>H NMR signals, as was discussed above.

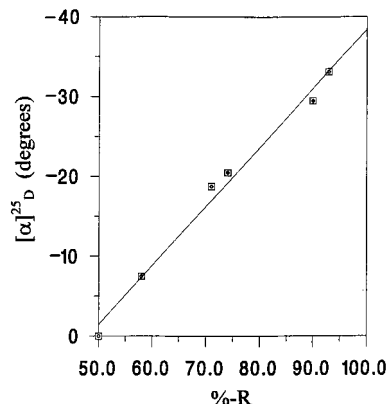
Previous research has shown that the polarity of solvents plays important roles in heterogeneous enzyme-catalyzed reactions in organic media.<sup>29–32</sup> However, models that satisfactorily explain or allow the prediction of solvent effects for specific PPL- or PS-30-substrate pairs are not as yet available. Thus, this paper will not attempt to provide rationalizations for the solvent effects observed herein.

**Chemical Polymerization of Enzyme-Resolved MPL and GPC Analyses.** Mixtures of 93% (*R*)-MPL and *rac*-MPL were used to prepare PMPL of variable enantiopurities. The results of the yield, molecular weight averages, and polydispersity of polymers formed from 50%, 58%, 71%, 74%, 90%, and 93% (*R*)-MPL using CH<sub>3</sub>COOK/dibenzo-18-crown-6 as initiator are summarized in Table 2. Polymer yields (based on insoluble product recovered from precipitation into methanol) ranged from 80% to 95% and *M<sub>n</sub>* values from 9300 to 16 300 g/mol (see Table 2). Furthermore, polydispersities (*M<sub>w</sub>*/*M<sub>n</sub>*) as low as 1.12 were achieved. Since the anionic initiated polymerization reaction mechanism for similar α-substituted β-propiolactone monomers is believed to occur via cleavage of the alkyl (β-CH<sub>2</sub>) carbon-oxygen bond<sup>8</sup> which does not involve bond reorganizations at the asymmetric center, it was expected that

**Table 2. Results on Yield and Molecular Weight of Synthesized PMPL Stereoisomers<sup>a</sup>**

product <sup>b</sup>	[M]/[I] <sup>c</sup>	yield, %	<i>M<sub>n</sub></i> <sup>f</sup>	<i>M<sub>w</sub></i> / <i>M<sub>n</sub></i> <sup>f</sup>
50% ( <i>R</i> )-PMPL	500	88 <sup>d</sup>	11 500	1.12
58% ( <i>R</i> )-PMPL	550	80 <sup>e</sup>	14 700	1.22
71% ( <i>R</i> )-PMPL	1080	91 <sup>e</sup>	16 300	1.24
74% ( <i>R</i> )-PMPL	450	90 <sup>e</sup>	10 600	1.25
90% ( <i>R</i> )-PMPL	500	86 <sup>e</sup>	12 800	1.36
93% ( <i>R</i> )-PMPL	750	95 <sup>e</sup>	9 300	1.59

<sup>a</sup> 60 °C, 4 days, CH<sub>3</sub>CO<sub>2</sub>K/dibenzo-18-crown-6 (1:2) as initiator. <sup>b</sup> The % (*R*) contents given for products are those measured by <sup>1</sup>H NMR analysis of the monomer feed. <sup>c</sup> [M]/[I] is the molar ratio of MPL to the CH<sub>3</sub>CO<sub>2</sub>K initiator component. <sup>d</sup> Product precipitated in methanol and isolated by centrifuge. <sup>e</sup> Product precipitated in methanol and isolated by vacuum filtration. <sup>f</sup> Determined by GPC.

**Figure 3.** Plot of  $[\alpha]^{25}_D$  (*c* 0.8 g/dL, CHCl<sub>3</sub>) vs % (*R*) content for a series of PMPL stereoisomers.

polymerization of optically active MPL occurs with complete retention of configuration. Thus, PMPL's having predominantly (*R*) repeat unit stereochemical configurations were formed, and the polymer stereochemical purity is assumed to be equivalent to that of the monomer feed. It is noteworthy to mention that GPC traces of PMPL stereoisomers showed unexpected complexity. Specifically, in addition to GPC peaks used for molecular weight measurements, the 50%, 58%, 71%, and 74% (*R*)-PMPL polymers all showed another peak at relatively shorter elution volumes that corresponded to products having molecular weights greater than  $1 \times 10^9$  g/mol. The relative area of these apparent high molecular peaks was between 20% and 40% of the total eluted peak area. This result may be rationalized by assuming that certain PMPL chain stereochemistries are able to form aggregates. Work is currently underway in our laboratory to test the validity of this interesting observation.

**Polarimetry.** A plot of specific rotation vs % (*R*) was constructed using PMPL stereoisomers that were synthesized having % (*R*) contents of 50%, 58%, 71%, 74%, 90%, and 93%, respectively (see Figure 3). It was found that a linear relationship exists between PMPL specific rotation and % (*R*) contents (correlation coefficient of 0.990) which, by extrapolation, gave a  $[\alpha]^{25}_D$  (*c* 0.8 g/dL, CHCl<sub>3</sub>) for 100% (*R*)-PMPL of -38.4°. Thus, the measured specific rotation appears to simply result from the additive contribution of chain enantiomeric repeat units. In other words, the optical rotation of repeat unit stereoisomers along the chain is not substantially affected by neighboring repeat units that are a function of chain enantiopurity. In a previous report,<sup>10</sup> a plot of PMPL  $[\alpha]^{25}_D$  vs % (*S*) content was presented which also showed a linear relationship. However, the value reported for the  $[\alpha]^{25}_D$  (concentration not reported, in

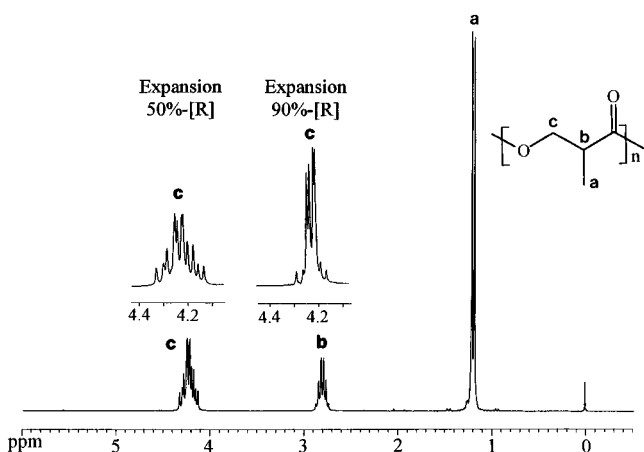


**Figure 4.**  $^1\text{H}$  NMR (250-MHz) spectrum in chloroform- $d$  of 50% (*R*)-PMPL along with expansions of the  $\beta$ -methylene proton signal region for 50% and 90% (*R*)-PMPL.

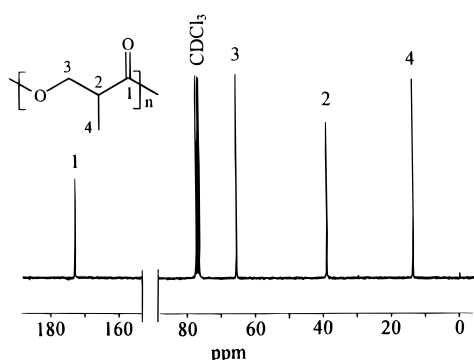


**Figure 5.**  $^{13}\text{C}$  NMR (62.9-MHz) spectrum in chloroform- $d$  of 50% (*R*)-PMPL.

$\text{CHCl}_3$ ) of 100% (*S*)-PMPL was  $+16.2^\circ$ , which is considerably lower than the value obtained herein.

**NMR Analyses of PMPL Stereoisomers.** The  $^1\text{H}$  NMR spectra at 250 MHz recorded in chloroform- $d$  of PMPL stereocopolymers were not useful for quantitation of diad (or higher) sequences but showed additional complexity (most readily observed for the  $\beta$ -methylene protons *c*) as the polymer enantiopurity decreased (see Figure 4). The 50%, 74%, and 93% (*R*)-PMPL samples were then analyzed at 62.9 MHz in chloroform- $d$  by  $^{13}\text{C}$  NMR. The full spectrum of 50% (*R*)-PMPL along with peak assignments is given in Figure 5, while expanded regions for the carbonyl (C-1), methine (C-2), and methyl (C-4) carbons are shown in Figure 6. It was found that C-1, C-2, and C-4 were sensitive to the effects of repeat unit sequence, while C-3 was not at this field strength. The diad sequences can be observed for both C-1 and C-4, while the triad sequences can be observed for C-2. The assignment of the diad sequences for C-1 and C-4 was carried out by comparing the relative intensities of the two observed signals where the expectation is that the isotactic (*i*) diad signal will increase relative to the syndiotactic (*s*) diad signal with an increase in the % (*R*) content of PMPL. The triad sequences for C-2 were assigned based on the following: (1) isotactic (*ii*) triads were identified as the upfield signal since it was the dominant signal for the 93% (*R*)-PMPL sample; (2) syndiotactic (*ss*) triads were assigned based on their relative peak intensities, which agreed with that calculated by the Bernoulli model for the 50% (*R*)-PMPL sample (see discussion below and Table 3); (3) heterotactic (*is* and *si*) triads were assigned as was described in 2 and with the assumption that these triads would

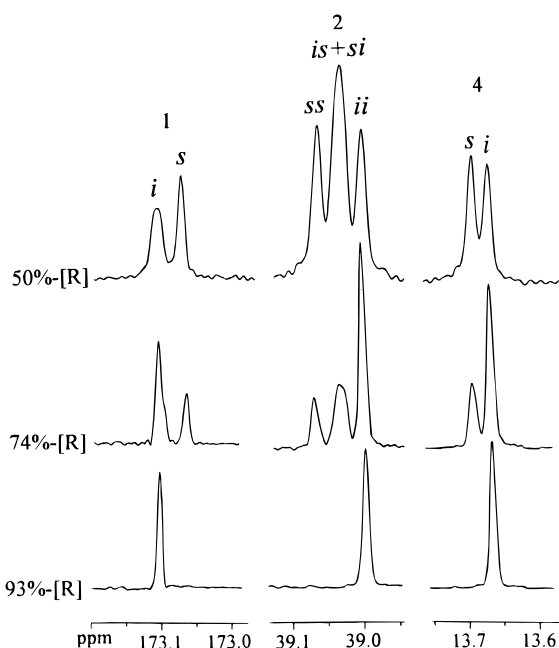


**Figure 6.** Expanded regions of 62.9 MHz  $^{13}\text{C}$  NMR spectra recorded for 50%, 74%, and 93% (*R*)-PMPL products.

**Table 3.** Chain Sequences of Stereocopolymers 50%, 74%, and 93% (*R*)-PMPL Determined by  $^{13}\text{C}$  NMR

product	diad <sup>a,c</sup>		triad <sup>b,c</sup>			<i>E</i> <sup>d,e</sup>
	<i>i</i>	<i>s</i>	<i>ii</i>	<i>ss</i>	<i>is + si</i>	
50% ( <i>R</i> )-PMPL	0.49 (0.50)	0.51 (0.50)	0.24 (0.25)	0.26 (0.25)	0.50 (0.50)	
74% ( <i>R</i> )-PMPL	0.71 (0.62)	0.29 (0.38)	0.54 (0.42)	0.15 (0.19)	0.31 (0.39)	0.97
93% ( <i>R</i> )-PMPL	1.00 (0.87)	0.00 (0.13)	1.00 (0.80)	0.00 (0.07)	0.00 (0.15)	
			[1.00]	[0.00]	[0.00]	

<sup>a</sup> Diad fractions *i* (isotactic) and *s* (syndiotactic) were calculated from the relative areas of the carbonyl  $^{13}\text{C}$  NMR signals. <sup>b</sup> Triad fractions *ii* (isotactic), *ss* (syndiotactic), and *is + si* (heterotactic) were calculated from the relative areas of the methine  $^{13}\text{C}$  NMR signals. <sup>c</sup> Values in parentheses were calculated from the enantiopurities of the monomer feeds using Bernoulli equations (see ref 34). Values in brackets were calculated using the enantiomeric-site model equations (see refs 35–37). <sup>d</sup> Enantiomeric-site model triad test  $E = 2ss/(is + si) = 1$  for a polymer perfectly described by the enantiomeric-site model. <sup>e</sup> *E* value for 93% (*R*)-PMPL cannot be calculated due to the absence of the *s* and *is + si* peaks.

be poorly resolved due to the small effects of ester bond directionality on differences in *is* and *si* chemical shifts.<sup>33</sup> Inspection of Table 3 shows that the 50% (*R*)-PMPL diad and triad fraction results obtained experimentally fit the Bernoulli model for ideal random chain propagation<sup>34</sup> (see Table 3 legends *a* and *c*). In contrast, for the 74% and 93% (*R*)-PMPL samples, it is clear by comparison of the diad and triad fractions obtained experimentally and by calculation using the Bernoulli model that chain propagation is no longer proceeding by ideal random propagation statistics. In fact, there appears to be a tendency toward isospecificity based on the fact that the experimental *i* diad and *ii* triad fractions are substantially greater than those calculated by the Bernoulli model (see Table 3). In fact, the 93% (*R*)-PMPL sample did not show observable peaks due to *s* diad and *ss* and *si + is* triads (see Figure 6). The triad data for the 74% and 93% (*R*)-PMPL were also evaluated by the enantiomeric-site model (see Table 3, legends *c* and *d* and refs 35–37). Interestingly, using

**Table 4.** DSC Measurements of PMPL Stereoisomers<sup>a</sup>

product	$T_g$ , <sup>b</sup> °C	$T_m$ , <sup>c</sup> °C	$\Delta H_f$ , <sup>d</sup> cal/g
50% ( <i>R</i> )-PMPL	-30		
58% ( <i>R</i> )-PMPL	-27	42	3.8
71% ( <i>R</i> )-PMPL	-25	65	10.0
74% ( <i>R</i> )-PMPL	-26	77	14.7
90% ( <i>R</i> )-PMPL	-25	130	20.7
93% ( <i>R</i> )-PMPL	-24	131	22.0

<sup>a</sup> See Experimental Section for detailed description of the method used. <sup>b</sup> The midpoint values measured after rapidly quenching the sample from the melt and recording the second heating scan. <sup>c</sup> Taken from first heating scans of solution precipitated products. The value reported is the peak melting temperature of the largest endotherm transition. <sup>d</sup> The cumulative value over the entire melting region.

this model, it was found that there was excellent agreement between calculated and experimental triad fractions for the 74% (*R*)-PMPL and 93% (*R*)-PMPL samples (see Table 3). The triad test *E* value for the 93% (*R*)-PMPL sample was not calculated by the enantiomorphous-site model since the values of the *s* diad and *ss* and *is* + *si* triads were below the instrument detection limit. The enantiomorphous-site model assumes that the configuration of monomer adding to a chain end is determined primarily by the configuration of the catalyst and is not directed by the chain end configuration.<sup>35</sup> However, previous work has suggested that the catalyst CH<sub>3</sub>COOK/dibenzo-18-crown-6 is nonstereoregulating.<sup>10</sup> That the CH<sub>3</sub>COOK/dibenzo-18-crown-6 catalyst appears to be nonstereoregulating for the racemic MPL polymerization but is isoregulating for the enantioenriched MPL polymerization is interesting. It may be speculated that the catalyst, when chelated by predominantly one MPL enantiomeric form, takes on a chiral microenvironment that leads to isospecific catalysis. Future work will be carried out to further study this unexpected result.

**Thermal Analysis.** The solution-precipitated PMPL stereoisomers were characterized by DSC (see Experimental Section). The results obtained for  $T_g$ ,  $T_m$ , and  $\Delta H_f$  are tabulated in Table 4 and the DSC thermograms for the first and second heating scans are shown in Figure 7a and 7b, respectively.  $T_g$  values measured from the second heating scans decreased from -24 to -30 °C with a decrease in the polymer enantiopurity from 93% to 50% (*R*). Thus, it appears that higher chain isotacticity results in increased chain rigidity. The 50% (*R*)-PMPL, which approximates a statistically random copolymer, was amorphous (no observed melting transition, see Figure 7), consistent with a previous report.<sup>10</sup> However, 58% (*R*)-PMPL has a melting transition with  $T_m$  and  $\Delta H_f$  values of 42 °C and 3.8 cal/g, respectively (see Table 4 and Figure 7a). This indicates that relatively low *i* diad fractions are required for PMPL crystallization. By increasing the % (*R*) content of PMPL to 93%, the  $T_m$  and  $\Delta H_f$  values increased to 131 °C and 22.0 cal/g, respectively (see Table 4 and Figure 7a). In a previous report by Hmamouchi and Prud'homme,<sup>10</sup> an (*S*)-PMPL sample which was believed to be enantiopure had  $T_m$  and  $\Delta H_f$  values of 80 °C and 14.6 cal/g, respectively, which are similar values to those reported herein for the 74% (*R*)-PMPL sample. The relatively higher degree of PMPL crystalline ordering shown herein relative to that previously reported<sup>10</sup> is believed to be due to the overestimations by those workers of MPL enantiopurity (see above). The 90% and 93% (*R*)-PMPL products crystallized rapidly on heating during the second scans (see Figure 7b) at

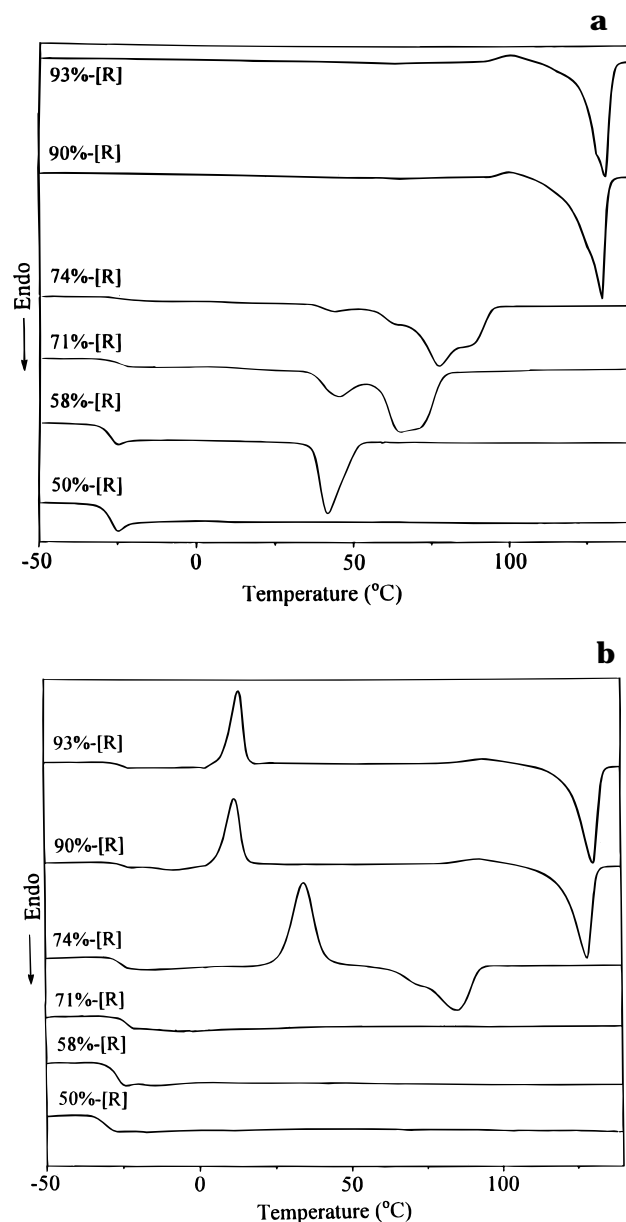


**Figure 7.** DSC thermograms recorded for PMPL stereoisomers: (a) first heating scans and (b) second heating scans after rapid quenching from the melt.

temperatures of 12 and 13 °C, respectively, indicating that PMPL may have desirable crystallization kinetics.

It is interesting to compare the thermal properties of PMPL stereocopolymers to those of PHB and PLA stereocopolymers. In previous studies by Tanahashi and Doi<sup>38</sup> and Kemnitzer *et al.*,<sup>39</sup> PHB ideal random stereocopolymers have been prepared and analyzed by DSC. Tanahashi and Doi reported that solution-precipitated 92% (*S*)-PHB ( $M_n$  34 000,  $M_w/M_n = 1.5$ ) had  $T_m$  and  $\Delta H_f$  values of 136 °C and 15.4 cal/g, respectively.<sup>38</sup> Kemnitzer *et al.* showed that 67% (*R*)-PHB ( $M_n$  7000,  $M_w/M_n = 1.1$ ) had  $T_m$  and  $\Delta H_f$  values of 50 °C and 2 cal/g, respectively.<sup>39</sup> Inspection of Table 4 shows that PMPL samples having 90% and 58% (*R*) contents most closely approximate the thermal transitions of 92% (*S*)- and 67% (*R*)-PHB. Without additional comparative data points and knowledge of the PMPL crystal structure, our conclusions at present are limited to the following: (1) both PHB and PMPL have considerable tolerance to stereochemical impurities so that crystallization is possible for these polymer structural isomers

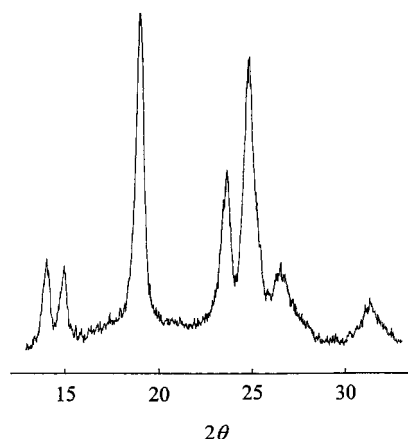


**Figure 8.** WAXS pattern of 90% (*R*)-PMPL crystallized by melt-annealing at 100 °C.

at low polymer enantiopurities, and (2) PMPL, having a similar range of melting temperatures to PHB, can be obtained via the appropriate variation in chain enantiopurity. In contrast, PLA stereocopolymers have a much lower tolerance to stereochemical impurities. For example, [L]-/[D]-lactide and [L]-/*meso*-lactide random stereocopolymers which have only 12% and 10% [D]-lactic acid repeat units, respectively, do not crystallize.<sup>40</sup>

**X-ray Diffraction Analysis.** WAXS data collected for 90% (*R*)-PMPL, which was crystallized by annealing from the melt at 100 °C (see Experimental Section), are shown in Figure 8. The WAXS pattern shows well-resolved crystalline reflections superimposed on a low-intensity amorphous halo. This indicates high levels of crystallinity and uniformly organized crystals. The degree of crystallinity,  $\chi_c$ , was estimated to be 73% from diffracted intensity data by dividing the area of the crystalline peaks by the total area of the crystalline peaks and amorphous scattering (see Experimental Section). Thus, it appears that the % crystallinity of 90% (*R*)-PMPL is high and similar in value to natural P3HB (60–74%).<sup>41</sup> The major diffraction peaks at  $2\theta = 14.0, 14.8, 19.0, 23.8, 25.0, 26.6,$  and  $31.6^\circ$  correspond to *d*-spacings of 6.35, 5.94, 4.67, 3.74, 3.56, 3.34, and 2.83 Å, respectively. With the exception of the *d* spacing at 6.35 Å, these values are in excellent agreement with the *d* spacings previously reported for (*S*)-enriched PMPL.<sup>10</sup>

**FTIR Analysis.** Crystallinity sensitive IR bands have been identified for natural PHB and related copolyesters and used to follow sample crystallization.<sup>24</sup> Specifically, significant changes in the absorption bands at 1279, 1228, and 1185  $\text{cm}^{-1}$  were observed due to crystallization where the band at 1385  $\text{cm}^{-1}$  was considered crystalline insensitive. Later, in our laboratory, it was found that the appearance of a band at 1206  $\text{cm}^{-1}$  with a concurrent decrease in intensity at 1180  $\text{cm}^{-1}$  and an increase in the band intensity at 1103  $\text{cm}^{-1}$  are spectral features that allow crystalline syndiotactic PHB to be distinguished from its atactic and isotactic stereoisomers.<sup>43</sup> Based on the above, work was undertaken to determine crystalline-sensitive bands for PMPL in the 700–1600- $\text{cm}^{-1}$  spectral region. FTIR spectra were recorded of 74% (*R*)-PMPL after melting at  $\sim 90^\circ\text{C}$  and annealing at room temperature for <1 min (broken line) and 20 h (solid line) (see Figure 9a). Great care was taken in this work so that the sample placement relative to the beam was identical so as to not introduce differences in observed sample concentration as a func-

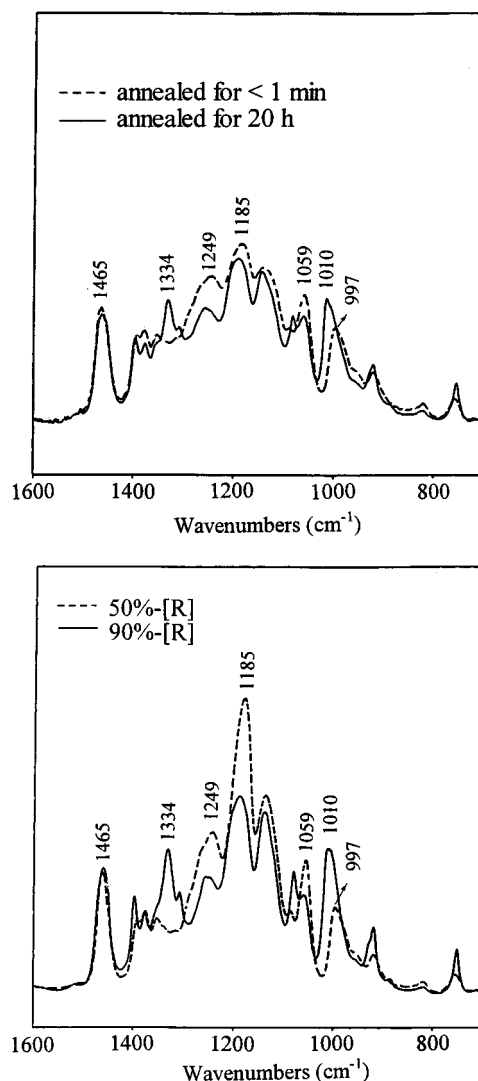


**Figure 9.** FTIR spectra: (a) 74% (*R*)-PMPL which was melt annealed at room temperature for <1 min and 20 h, (b) 90% (*R*)-PMPL which was melt-annealed at 100 °C and amorphous 50% (*R*)-PMPL.

tion of annealing time. It is expected that annealing for 20 h relative to 1 min will lead to a sample of higher crystallinity. The most notable differences that occur at higher PMPL crystallinity are the development of a new band at 1334  $\text{cm}^{-1}$ , decreased intensity of the 1249- and 1185- $\text{cm}^{-1}$  bands, a decrease in the band intensity at 1059  $\text{cm}^{-1}$ , and a shift in the absorbance maximum at 997–1010  $\text{cm}^{-1}$  with a concurrent increase in band intensity. The vibrational band at 1465  $\text{cm}^{-1}$  appeared to be crystallinity insensitive (see Figure 9a). It is interesting to note that crystallization of natural PHB also resulted in a decreased intensity of the vibrational band at 1185  $\text{cm}^{-1}$ .<sup>42</sup> To further verify the spectral features of crystalline PMPL, FTIR spectra in Figure 9b of 90% (*R*)-PMPL (solid line) which was melt annealed at 100 °C and amorphous 50% (*R*)-PMPL (broken line) are displayed (see Experimental Section for additional details on sample preparation). The two spectra in Figure 9b were normalized to take into account the differences in sample concentration by using the 1463- $\text{cm}^{-1}$  crystalline-insensitive band. As anticipated, the changes in spectral features observed in Figure 9b due to sample crystallinity were identical to those observed in Figure 9a except that the differences between spectra in Figure 9b were greater due to the high crystallinity of 90% (*R*)-PMPL (see Figures 7a and 8 and Table 4).

Based on the above, PMPL crystallization could be monitored using FTIR by taking a ratio of the bands at either 1334, 1010, or 1185  $\text{cm}^{-1}$  relative to the crystallization-insensitive band at 1465  $\text{cm}^{-1}$ .

### Summary of Results

Based on comparative studies with different lipases, PS-30 was found to be a suitable catalyst to resolve racemic MPL where the (*S*) enantiomer reacts more rapidly with methanol and benzyl alcohol. By this route, MPL was obtained, having up to 93% (*R*) content. MPL polymerization was then carried out using  $\text{CH}_3\text{COOK}$ /dibenzo-18-crown-6 as the catalyst so that a chemoenzymatic strategy was employed for the transformation of racemic MPL to high enantiopurity PMPL. Analysis by  $^{13}\text{C}$  NMR showed that the carbonyl, methine, and methyl carbons of PMPL are sensitive to stereochemical sequences along the chain. While the polymerization of 50% (*R*)-MPL followed Bernoulli random chain propagation statistics, polymerizations of 74% and 93% (*R*)-MPL deviated from the Bernoulli model. Further analysis showed that these latter polymerizations fit the enantiomorphic-site model. While the origin of these results is not as yet understood, isoregulating characteristics of the  $\text{CH}_3\text{COOK}$ /dibenzo-18-crown-6 catalyst for enantioenriched MPL polymerizations were demonstrated. By increasing the % (*R*) content in the monomer feed to 93%, a product was obtained which, from DSC measurements, had  $T_m$  and  $\Delta H_f$  values of 131 °C and 22.0 cal/g, respectively. Furthermore, WAXS analysis carried out on a melt-annealed 90% (*R*)-PMPL sample showed that the polymer was highly crystalline (approximately 73%). FTIR analysis identified crystalline-sensitive vibrational bands which will be useful for monitoring PMPL crystallization kinetics.

**Acknowledgment.** We are grateful for the financial support of this work by the Polymer Degradation Research Center at the University of Massachusetts—Lowell; the U.S. Army Natick RD&E Center, Natick, MA (Contract No. DAAK60-93-K-0010); and the Rohm & Haas Co. Also, we thank Mr. Michael Downey for performing the WAXS measurement.

### References and Notes

- (1) For reviews, see: Gross, R. A. In *Biomedical Polymers: Designed to Degrade Systems*; Shalaby, S. W., Ed.; Hanser: New York, 1994; pp 2–19. Steinbüchel, A. In *Biomaterials: Novel Materials from Biological Sources*; Byrom, D., Ed.; Stockton: New York, 1991; p 123–213. Doi, Y. *Microbial Polyesters*; VCH: New York, 1990. Brandl, H.; Gross, R. A.; Lenz, R. W.; Fuller, R. C. In *Advances in Biochemical Engineering/Biotechnology*; Fiechter, Ed.; Springer-Verlag: Berlin, Heidelberg, 1990; Vol. 41, p 77.
- (2) Vert, M.; Christel, P.; Chabot, F.; Leray, J. In *Macromolecular Biomaterials*; Hastings, G. W., Ed.; Ducheyne, P., CRC: Boca Raton, FL, 1984; pp 119–142.
- (3) Zhang, X.; Goosen, M. F. A.; Wyss, U. P.; Pichora, D. *J.M.S.-REV, Macromol. Chem. Phys.* **1993**, C33 (1), 81.
- (4) Mayer, J.; Kaplan, D. L. *Trends Polym. Sci.* **1994**, 2, 227.
- (5) Lenz, R. W. *Adv. Polym. Sci.* **1993**, 107, 3.
- (6) Hmamouchi, M.; Prud'homme, R. E. *J. Polym. Sci., Polym. Chem. Ed.* **1991**, 29, 1281.
- (7) Carriere, F. J.; Eisenbach, C. D. *Makromol. Chem.* **1981**, 182, 325.
- (8) D'hondt, C. G.; Lenz, R. W. *J. Polym. Sci., Polym. Chem. Ed.* **1978**, 16, 261.

- (9) Grenier, D.; Prud'homme, R. E. *J. Polym. Sci., Polym. Chem. Ed.* **1981**, 19, 1781.
- (10) Hmamouchi, M.; Prud'homme, R. E. *J. Polym. Sci., Polym. Chem. Ed.* **1988**, 26, 1593.
- (11) For reviews see: Whitesides, G. M.; Wong, C. H. *Angew. Chem., Int. Ed. Engl.* **1985**, 24, 217. Klibanov, A. M. *CHEMTECH* **1986**, 16, 354. Dordich, J. S. *Enzyme Microb. Technol.* **1989**, 11, 194.
- (12) Fellous, R.; Lizzani-Cuvelier, L.; Loiseau, M. A.; Sassy, E. *Tetrahedron: Asymm.* **1994**, 5, 343.
- (13) Blanco, L.; Guibe-Jampel, E.; Rousseau, G. *Tetrahedron Lett.* **1988**, 29, 1915.
- (14) Guibe-Jampel, E.; Rousseau, G.; Blanco, L. *Tetrahedron Lett.* **1989**, 30, 67.
- (15) Zaks, A.; Klibanov, A. M. *J. Am. Chem. Soc.* **1984**, 106, 2687.
- (16) Wilson, W. K.; Baca, S. B.; Barber, Y. J.; Scallen, T. J.; Morrow, C. J. *J. Org. Chem.* **1983**, 48, 3960.
- (17) Gutman, A. L.; Zuobi, K.; Bravdo, T. *J. Org. Chem.* **1990**, 55, 3546.
- (18) Gutman, A. L.; Oren, D.; Boltanski, A.; Bravdo, T. *Tetrahedron Lett.* **1987**, 28, 5367.
- (19) Gutman, A. L.; Zuobi, K.; Bravdo, T. *Tetrahedron Lett.* **1987**, 28, 3861.
- (20) Chen, X.; Dordick, J. S.; Rethwisch, D. G. *Macromolecules* **1995**, 28, 6014 and references therein.
- (21) MacDonald, R. T.; Pulapura, S. K.; Svirkin, Y. Y.; Gross, R. A.; Kaplan, D. L.; Akkara, J.; Swift, G.; Wolk, S. *Macromolecules* **1995**, 28, 73.
- (22) Silverstein, R. M.; Bassler, G. C.; Morrill, T. C. *Spectrometric Identification of Organic Compounds*, 4th ed.; John Wiley & Sons: New York, 1981; Chapter 6.
- (23) Slomkowski, S.; Penczek, S. *Macromolecules* **1980**, 13, 229.
- (24) Bloembergen, S.; Holden, D. A.; Hamer, G. K.; Bluhm, T. L.; Marchessault, R. H. *Macromolecules* **1986**, 19, 2865.
- (25) Chen, C. S.; Fujimoto, Y.; Girdaukas, G.; Sih, C. J. *J. Am. Chem. Soc.* **1982**, 104, 7294.
- (26) Chen, C. S.; Wu, S. H.; Girdaukas, G.; Sih, C. J. *J. Am. Chem. Soc.* **1987**, 109, 2812.
- (27) The theoretical curves were in excellent agreement with experimentally obtained ee vs conversion results so that MPL resolution by PPL occurs by a mechanism that agrees with the assumptions used for the derivation of eq 2 given in refs 25 and 26.
- (28) Svirkin, Y. Y.; Xu, J.; Gross, R. A.; Kaplan, D. L.; Swift, G. *Macromolecules* **1996**, 29, 4591–4597.
- (29) Klibanov, A. M. *Acc. Chem. Res.* **1990**, 23, 114.
- (30) Sakurai, T.; Margolin, A. L.; Russell, A. J.; Klibanov, A. M. *J. Am. Chem. Soc.* **1988**, 110, 7236.
- (31) Kitaguchi, H.; Fitzpatrick, P. A.; Huber, J. E.; Klibanov, A. M. *J. Am. Chem. Soc.* **1989**, 111, 3094.
- (32) Laane, C.; Boeren, S.; Veeger, C. *Biotech. Bioeng.* **1987**, 30, 81.
- (33) Kemnitzer, J. E.; McCarthy, S. P.; Gross, R. A. *Macromolecules* **1993**, 26, 1221.
- (34) The diad and triad fractions for the Bernoulli model can be calculated with knowledge of the monomer stereochemical composition (fraction of (*R*)- and (*S*)-MPL) using the following relationships:  $i = [R]^2 + [S]^2$ ;  $s = 2[R][S]$ ;  $ii = [R]^3 + [S]^3$ ;  $is = si = ss = [R][S]$ . See: Sepulchre, M. *Makromol. Chem.* **1988**, 189, 1117.
- (35) For the enantiomorphic-site model, the triads were calculated using the following equations:  $ii = 1 - 3s/2$ ;  $is + si = s$ ;  $2ss = s$ , where  $i$  and  $s$  were obtained experimentally as described in Table 3 legend a. See: Shelden, R. A.; Fueno, T.; Tsunetsugu, T.; Furukawa, J. *Polym. Lett.* **1965**, 3, 23.
- (36) Ewen, J. A. *J. Am. Chem. Soc.* **1984**, 106, 6355.
- (37) Hocking, P. J.; Marchessault, R. H. *Macromolecules* **1995**, 28, 6401.
- (38) Tanahashi, N.; Doi, Y. *Macromolecules* **1991**, 24, 5732.
- (39) Kemnitzer, J. E.; McCarthy, S. P.; Gross, R. A. *Macromolecules* **1992**, 25, 5927.
- (40) MacDonald, R. T.; McCarthy, S. P.; Gross, R. A. Manuscript in preparation.
- (41) Bluhm, T. L.; Hamer, G. K.; Marchessault, R. H.; Fyfe, C. A.; Veregin, R. P. *Macromolecules* **1986**, 19, 2872.
- (42) Kemnitzer, J. E.; Gross, R. A.; McCarthy, S. P.; Liggat, J.; Blundell, D. J.; Cox, M. *J. Environ. Polym. Deg.* **1995**, 3 (1), 37.

MA951869I